



## Preparation and characterization of high embedding efficiency epigallocatechin-3-gallate glycosylated nanocomposites

Jianyong Zhang<sup>a,b,1</sup>, Hongchun Cui<sup>c,1</sup>, Jiahuan Qiu<sup>b</sup>, Yixin Zhong<sup>b</sup>, Caiping Yao<sup>b</sup>, Lanying Yao<sup>b</sup>, Qunxiong Zheng<sup>b</sup>, Chunhua Xiong<sup>b,\*</sup>

<sup>a</sup> Tea Research Institute, Chinese Academy of Agricultural Science, Hangzhou, 310008, PR China

<sup>b</sup> Department of Applied Chemistry, Zhejiang Gongshang University, Hangzhou, 310012, PR China

<sup>c</sup> Tea Research Institute, Hangzhou Academy of Agricultural Science, Hangzhou, 310024, PR China

### ARTICLE INFO

#### Keywords:

Epigallocatechin-3-gallate  
Carboxymethyl chitosan  
Peanut globin  
Casein  
Glycosylation

### ABSTRACT

Glycosylated protein nano encapsulation was an efficient encapsulation technology, but its embedding rate for EGCG was not high, and the research on the embedding mechanism was relatively weak. Based on this, this study compared the embedding effect of glycosylated peanut globulin and glycosylated casein on EGCG. The embedding mechanism of EGCG with glycosylated protein was discussed by ultraviolet, fluorescence, infrared and fluorescence microscopy. Results revealed that the highest encapsulation efficiency of EGCG was  $93.89 \pm 1.11\%$ . The neutral pH value and 0.3 mg/mL EGCG addition amount were suitable for EGCG glycosylated nanocomposites. The hydrogen bond between EGCG hydroxyl group and tyrosine and tryptophan of glycosylated protein is mainly non covalent. The encapsulation effect of EGCG glycosylated nanocomposites could be quenched by changing the polar environment and spatial structure of the group. The fluorescence characteristic and dispersibility of EGCG glycosylated peanut globin were higher than EGCG glycosylated casein. This study might provide a theoretical basis for EGCG microencapsulation technology and EGCG application in tea beverage and liquid tea food systems.

### 1. Introduction

(-)-Epigallocatechin-3-gallate (EGCG) is very important functional compound in tea catechins, accounting for more than 50%. EGCG has a variety of biological activities, which contains antioxidant, anti-cancer, anti-inflammatory, etc (Shtay et al., 2019). However, EGCG is very unstable in neutral or alkaline environment, which was sensitive to light, heat and oxygen (Yang et al., 2018). The stability and slow-releasing potential of EGCG can be improved by nanocomposite technology in food processing (Chen et al., 2019; Huang et al., 2020). Nanocomposite technology is an important research field in recent years, which provide new ideas for efficient development and utilization of food (Zhang et al., 2019; Mu et al., 2021; Zhan et al., 2022). Nanocomposite technology aim to slow down the loss of nutrients and functional components caused by light, heat, oxygen (Wang et al., 2022; Vesperini et al., 2017). At the same time, nanocomposite technology also can control the release of target nutrients and functional components at certain condition (Dai et al., 2020; Latnikova and Jobmann,

2017). Proteins and polysaccharides are often used as wall materials for nanocomposites in food industry. However, protein have such defects as low solubility, poor thermal stability, poor acid-base stability, micellar precipitation and precipitation. With only protein as the embedding wall material, the microcapsulation target embedding efficiency and stability are relatively poor (Chang and Nickerson, 2018). Moreover, polysaccharides have poor film-forming and emulsifying properties and cannot effectively protect sensitive target components (Sieminska-Kuczer et al., 2022). Therefore, using polysaccharides alone as nanocomposite wall materials have greater limitations. It can be seen that no matter which wall material was used singly, it can not adapt to complex food processing environment. The development and application of composite wall materials of sugars and proteins become a research hotspot for more researchers.

Proteins glycosylation can effectively solve above application problems of single nanocomposite wall materials (Abdelmoneem et al., 2018). Glycosylated protein can improve the thermal stability, emulsification, dispersibility, solubility of protein (Dridi and Bordenave,

\* Corresponding author.

E-mail address: [xiongch@163.com](mailto:xiongch@163.com) (C. Xiong).

<sup>1</sup> Jianyong Zhang, Hongchun Cui contributed equally to this work.

2021). Proteins glycosylation reaction is a green and efficient chemical modification method, which can spontaneously complete the reaction by heating (Chang et al., 2022). The proteins involved in glycosylation reaction are peanut globulin, casein, bovine albumin,  $\alpha$ -lactalbumin etc. Peanut globulin is an ideal green biodegradable material for nanocomposite preparation, which have good solubility, emulsifying stability, water retention and thermal stability (Pan et al., 2022). Casein have good thermal stability, emulsification and surface activity, which have been used as load wall material of nutrients (Du et al., 2022). Our research team have used peanut globulin and casein as the core and carboxymethyl chitosan as the shell to carry out maillard grafting reaction to obtain glycosylated peanut globulin and glycosylated casein, which improve the dispersibility and solubility of peanut globulin and casein, and alleviate the aggregation of protein (Qiu et al., 2018). Based on this, the embedding effect and mechanism of glycosylated peanut globulin and glycosylated casein on EGCG have been compared and analyzed in order to obtain a new method for preparing EGCG nanocomposites with high embedding rate in this research.

Many studies have proved that EGCG can react with polysaccharides and proteins in a non covalent and covalent manner, and formed stable nanocomposite complexes through self-assembly process, which can improve the solubility and stability of EGCG (Wang et al., 2019; Dridi and Bordenave, 2021). Non covalent interaction mainly involve hydrogen bond, hydrophobic bond, van der Waals force and ionic bond, among which hydrophobic bond and hydrogen bond are the main forces. The covalent mode of action is mainly mediated by the o-quinone mechanism of enzymatic or non enzymatic oxidation. The binding efficiency of EGCG, polysaccharides and proteins is affected by EGCG concentration, spatial structure, concentration, pH value, temperature, ionic strength, etc (Liang et al., 2016; Sieminska-Kuczer et al., 2022; Parolia et al., 2022). The maximal encapsulation of EGCG by EGCG-loaded solid lipid nanoparticles is 68.5%, which successfully protect the encapsulated EGCG along the storage period as well as under the adverse conditions at neutral pH values (Shtay et al., 2019). The chitosan-coated EGCG-hordein nanoparticles have been fabricated by layer-by-layer electrostatic stacking method for improving solubility and stability of EGCG, and encapsulation efficiency of EGCG is 87.3% (Song et al., 2022). In a word, the solubility and stability of EGCG are significantly improved after embedding. However, the encapsulation efficiency of EGCG is not high (Shtay et al., 2019; Song et al., 2022). Therefore, it is urgent to find a new embedding method and study its embedding mechanism.

It have been proved that glycosylated peanut globulin and glycosylated caseins had good solubility, thermal stability, which were good microcapsulation material (Qiu et al., 2018). Therefore, this research aims to explore new preparation methods of EGCG nanocomposites by glycosylated peanut globulin and glycosylated casein are compared, especially those with high encapsulation efficiency. The interaction mechanism and structural changes between EGCG and glycosylated proteins have been analyzed by means of FT-IR and fluorescence. We hope to provide a theoretical basis for EGCG nanocomposites technology and EGCG application in food industry.

## 2. Materials and methods

### 2.1. Materials

EGCG (purity 98%) was purchased from Shanghai Yuanye Biotechnology Co., Ltd (Shanghai, China). Disodium hydrogen phosphate (purity 100%) and disodium dihydrogen phosphate (purity 100%) were purchased from Aladdin Biochemical Technology Co., Ltd (Shanghai, China). Acetonitrile (purity 100%), glacial acetic acid (purity 100%), potassium bromide (purity 100%), rhodamine B (purity 100%), phosphoric acid (purity 100%) was purchased from Shanghai McLean Biochemical Technology Co., Ltd (Shanghai, China). Anhydrous ethanol (purity 100%) was purchased from Xilong Science Co., Ltd (Shantou,

China). Sodium hydroxide (purity 100%) was purchased from Sino-pharm Chemical Reagent Co., Ltd (Shanghai, China).

### 2.2. Preparation of glycosylated copolymer of peanut globulin and casein

The peanut protein and carboxymethyl chitosan (1:1, w/w), casein and carboxymethyl chitosan (1:1, w/w) were separately dissolved in phosphate buffer solution at pH 7.6, 4.8 mmol/L. The above solutions were separately treated with microwave at 220 W for 20 min and initial temperature 85 °C (XH-300UL-2 microwave catalytic synthesizer, Beijing Xianghu Technology Development Co., Ltd., China). The samples were pre-frozen in vacuum freeze-dryer for 6 h, and then sublimed and dried at 25 °C for 46 h by freeze dryer (LGJ50, Beijing Sihuan Pharmaceutical Co., Ltd., China). The dry samples was ground into powder manually by 50 mesh size. The powder samples were spread on the surface of the glass dishes. The glass dishes were put in a desiccators containing saturated potassium bromide at 60 °C for 3h. The samples were pre-frozen in vacuum freeze-dryer for 5 h, and then sublimed and dried at 25 °C for 39 h by freeze dryer (water catching capacity is 6 kg/day; freeze-drying area is 0.8 m<sup>2</sup>; LGJ50, Beijing Sihuan Pharmaceutical Co., Ltd., China). The peanut globulin glycosylation dry product and casein glycosylation dry product were obtained.

### 2.3. Effect of pH on the synthesis of EGCG loaded composite

The glycosylated peanut globulin and glycosylated casein were separately dissolved in 4.8 mmol/L phosphoric acid buffer solution. The pH values were 6.0, 6.5, 7.0, 7.5, and 8.0, respectively. Under this condition, the glycosylated peanut globulin and glycosylated casein were relatively stable. The solution was filtrated by filter paper (qualitative filter paper $\phi$ 9, Shanghai biyuntian biology technology co., ltd, china). In the unsealed state, 6 mL supernatant was respectively put into 10 mL sample glass bottle. 1 mg EGCG was added into 6 mL of the solution in parallel, which was sealed and stored in N<sub>2</sub> at 25 °C. The average particle size and polydisperse index (PDI) were quantized by Zetsizer nano-ZS90 analyzer (British Malvern Co.). The effect of pH on the formation of EGCG peanut globulin glycosylation copolymer (Ara-CMCS-EGCG) and EGCG casein glycosylation copolymer (Cas-CMCS-EGCG) were compared by average particle size and PDI. Duncan method in SPSS software was used to analyze the significance of differences between multiple pH groups of samples.

### 2.4. Effect of EGCG amount on the synthesis of carrier complex

6 mL peanut globulin glycosylation product solution and casein glycosylation product solution were separately filtered by filter paper. Different mass (1.0, 1.8, 3.6, 9.0 and 18 mg) of EGCG were added into the solution in parallel, which were sealed and stored in N<sub>2</sub> at 25 °C. The average particle size and polydisperse index (PDI) of Ara-CMCS-EGCG and Cas-CMCS-EGCG were employed to evaluation the effect of EGCG amount on the synthesis of carrier complex. Then, the Ara-CMCS-EGCG and Cas-CMCS-EGCG solvent were centrifugated at 4000 $\times$ g for 10 min at 4 °C by centrifuge equipment (5804R high speed refrigerated centrifuge, EPPENDORF Co., Ltd., Germany). The content of free EGCG could be determined by HPLC to calculate the amount of entrapment filtration and loading. Duncan method in SPSS software was used to analyze the significance of differences between multiple EGCG content groups of samples. Encapsulation rate of EGCG and loading amount of glycosylated compound per unit were calculated by equation (1) and equation (2).

$$EA = \frac{(TAE - CFE)}{TAE} \times 100\% \quad \text{Equation (1)}$$

where EA was encapsulation rate of EGCG, TAE was total amount of EGCG, CFE was content of free EGCG.

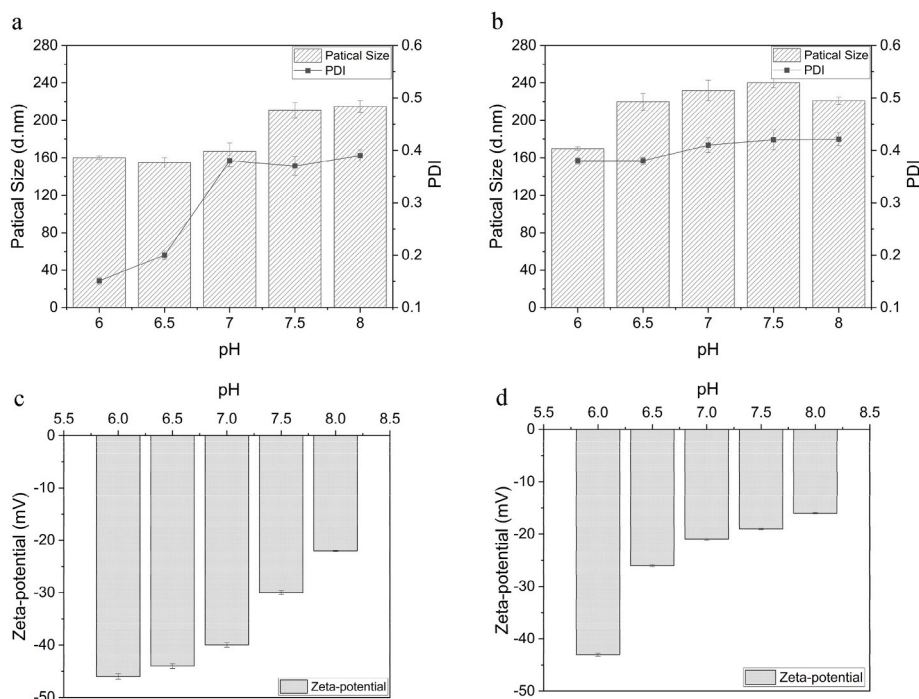


**Fig. 1.** The average size and PDI of Ara-CMCS-EGCG (a) and Cas-CMCS-EGCG (b), zeta-potential of Ara-CMCS-EGCG (c) and Cas-CMCS-EGCG (d) with different pH. Note: PDI was polydisperse index, Ara-CMCS-EGCG was EGCG peanut globulin glycosylation copolymer, Cas-CMCS-EGCG was EGCG casein glycosylation copolymer.

$$LU = \frac{LAE}{MGCC} \quad \text{Equation (2)}$$

where LU was loading amount of glycosylated compound per unit ( $\mu\text{mol}/\text{mg}$ ), LAE was loading amount of EGCG, MGCC was mass of glycosylated compound carrier.

## 2.5. HPLC detection conditions

The HPLC was Model Shimadzu LC-20A (Shimadzu Corporation, Kyoto, Japan). The chromatographic column was Sunfire C18 ( $5 \mu\text{m}$ ,  $4.6 \text{ mm} \times 250 \text{ mm}$ , Waters Corporation, USA). The HPLC injection volume was  $10 \mu\text{L}$ , and the column temperature was  $40 \text{ }^\circ\text{C}$ . The monitoring UV wavelength was set at  $280 \text{ nm}$ . The flow rate was  $1.0 \text{ mL}/\text{min}$ . Mobile phase A is  $0.2\%$  acetic acid, mobile phase B is  $100\%$  acetonitrile. The gradient for mobile phase A was set as follows:  $0\text{--}16 \text{ min}$ ,  $6.5\text{--}15\%$  A;  $16\text{--}20 \text{ min}$ ,  $15\text{--}25\%$  A;  $20\text{--}30 \text{ min}$ ,  $25\text{--}6.5\%$  A (Qiu et al., 2018).

## 2.6. Fluorescence spectrum analysis

The  $0.1$ ,  $0.2$ ,  $0.4$ ,  $0.6$ ,  $1.6$ ,  $5.4$ ,  $9.0 \text{ mg}$  EGCG were separately put into  $6 \text{ mL}$  glycosylated peanut globulin solution and glycosylated casein solution, which were sealed and stored in  $\text{N}_2$  at  $25 \text{ }^\circ\text{C}$ . The Ara-CMCS-EGCG and Cas-CMCS-EGCG were analyzed by fluorescence spectrometer.

Fluorescence spectrum analysis method (Qiu et al., 2018): fixed excitation wavelength  $\lambda$  was  $280 \text{ nm}$ . The excitation slit and emission slit were both  $5 \text{ nm}$ . The fluorescence scanning speed was  $300 \text{ nm}/\text{min}$ . The scanning range was  $290\text{--}450 \text{ nm}$ .

## 2.7. Infrared spectrum analysis of EGCG loaded composite

The ratio of the vacuum dried sample to KBr was  $1:50$ , which was ground under the irradiation of sodium lamp. The  $50\text{-mesh}$  ground solid powders were put into the die and pressed for about  $15 \text{ s}$  under  $20 \text{ MPa}$ . Then, the samples were put into the infrared spectrometer ( $400\text{--}4000 \text{ cm}^{-1}$ ) for full band scanning. The infrared spectrum result of the

samples was the superposition of 32 consecutive scans.

## 2.8. Fluorescence microanalysis by rhodamine B staining result

The  $1.8 \text{ mg}$  EGCG was separately added to the peanut globulin glycosylation product and casein glycosylation product in  $\text{N}_2$  at  $25 \text{ }^\circ\text{C}$ . The  $1 \text{ mL}$  samples were mixed with  $50 \mu\text{L}$  rhodamine B ( $0.2\%$  wt.). The nanostructures of Ara-CMCS-EGCG and Cas-CMCS-EGCG were analyzed under the fluorescence microscopy (Qiu et al., 2018).

## 2.9. Statistical analysis

The SPSS 20.0 (Chenna Inc., Chicago, USA) was used to process the data. All experiments were repeated in triplicates and the results were assessed by analysis of variance (ANOVA). The Student-Newman-Keuls test was used for pairwise comparisons of results, which were found to be significant by ANOVA. P values  $< 0.05$  were determined to be statistically significant. The software origin 8.1 was used to draw the picture.

## 3. Results and discussion

### 3.1. Effect of pH on the synthesis of Ara-CMCS-EGCG and Cas-CMCS-EGCG

The average particle size of Ara-CMCS-EGCG solution at pH  $6.0$  and Cas-CMCS-EGCG solution at pH  $6.0$  were relatively lower (Fig. 1.). The PDI of Cas-CMCS-EGCG solution was basically stable at pH  $6.0\text{--}8.0$ . The PDI of Ara-CMCS-EGCG solution at pH  $7.0$  became increased, which was likely due to the increase of pH value. With the increase of pH value, the zeta-potential of Ara-CMCS-EGCG and Cas-CMCS-EGCG decreased. When the solubility of Ara-CMCS-EGCG and cross-linking effect of EGCG increased, local aggregation occurred and uneven particle size distribution. With the increase of pH value, the average particle size of Ara-CMCS-EGCG and Cas-CMCS-EGCG increased firstly and then significantly decreased. The reason might be due to the change of the spatial structure of protein solution in the alkaline environment (Dai et al.,

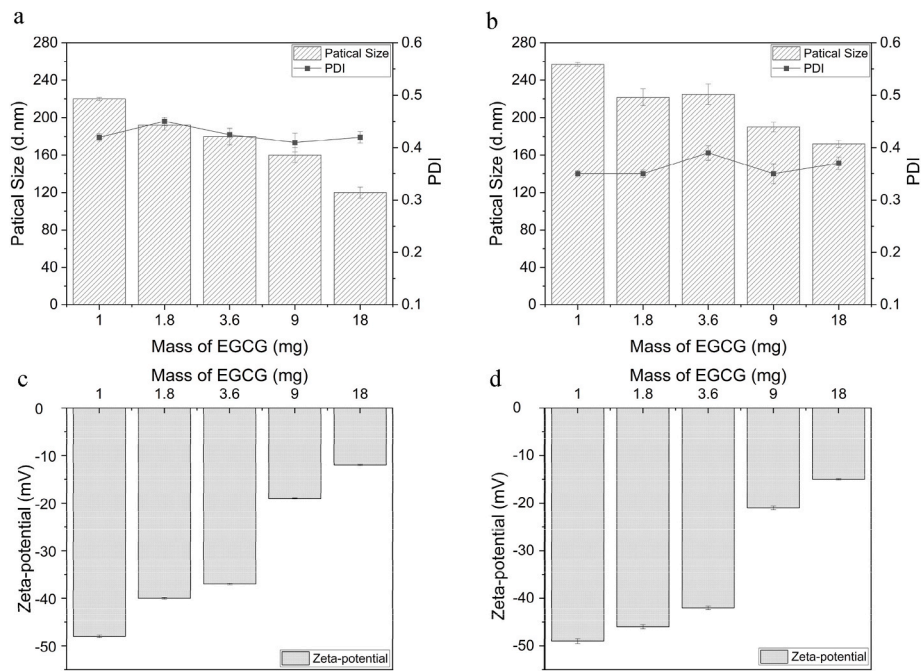


**Fig. 2.** The average size and PDI of Ara-CMCS-EGCG (a) and Cas-CMCS-EGCG (b), zeta-potential of Ara-CMCS-EGCG (c) and Cas-CMCS-EGCG (d) with different mass of EGCG addition.

Note: PDI was polydisperse index, Ara-CMCS-EGCG was EGCG peanut globulin glycosylation copolymer, Cas-CMCS-EGCG was EGCG casein glycosylation copolymer.

**Table 1**

Effect of different EGCG addition amount on the encapsulation efficiency of Ara-CMCS-EGCG and Cas-CMCS-EGCG.

| EGCG addition amount | Encapsulation efficiency (Ara-CMCS-EGCG) | EGCG loading amount (Ara-CMCS-EGCG) | Encapsulation efficiency (Cas-CMCS-EGCG) | EGCG loading amount (Cas-CMCS-EGCG) |
|----------------------|--|-------------------------------------|--|-------------------------------------|
| Mg                   | %  | μmol/mg                             | %  | μmol/mg                             |
| 1.0                  | 86.26 ± 1.17 <sup>a</sup>                | 52.27 ± 2.72 <sup>a</sup>           | 78.38 ± 1.05 <sup>b</sup>                | 71.24 ± 2.54 <sup>a</sup>           |
| 1.8                  | 91.05 ± 1.03 <sup>b</sup>                | 99.32 ± 1.75 <sup>b</sup>           | 79.68 ± 0.78 <sup>a</sup>                | 130.38 ± 3.33 <sup>b</sup>          |
| 3.6                  | 93.89 ± 1.11 <sup>c</sup>                | 204.83 ± 7.58 <sup>c</sup>          | 69.98 ± 1.13 <sup>e</sup>                | 229.01 ± 5.12 <sup>d</sup>          |
| 9.0                  | 91.04 ± 0.75 <sup>d</sup>                | 496.54 ± 11.13 <sup>d</sup>         | 60.82 ± 1.32 <sup>d</sup>                | 497.57 ± 10.79 <sup>e</sup>         |
| 18.0                 | 63.62 ± 1.68 <sup>e</sup>                | 693.98 ± 19.11 <sup>e</sup>         | 38.40 ± 2.51 <sup>c</sup>                | 628.31 ± 15.35 <sup>e</sup>         |

Note: Means of three measurements ± SD values with different letters are significantly different (p < 0.05), Ara-CMCS-EGCG was EGCG peanut globulin glycosylation copolymer, Cas-CMCS-EGCG was EGCG casein glycosylation copolymer.

2020), which tended to be loose and larger in the form of irregular folding (Wang et al., 2019). However, the average particle size decreased not significantly at pH 8.0, which might be caused by hydrolysis of some peptide amino acids in alkaline environment. EGCG was relatively stable in acid environment, and was easy to be oxidized and degraded to lose its activity in alkaline environment (Shtay et al., 2019). In weak acid environment, due to the closer cross-linking structure of EGCG, Ara-CMCS-EGCG and Cas-CMCS-EGCG molecules could exist stably in solution. In conclusion, pH 6.0 was selected as the optimal pH condition for the synthesis of Ara-CMCS-EGCG and Cas-CMCS-EGCG.

### 3.2. Effect of EGCG amount on the synthesis of Ara-CMCS-EGCG and Cas-CMCS-EGCG

The average particle size of Cas-CMCS-EGCG was significantly larger than that of Ara-CMCS-EGCG (Fig. 2.). EGCG had the function of bridging protein through hydrogen bond. Moreover, there was the electrostatic interaction between EGCG and protein. With the continuous addition of EGCG, the average particle size and zeta-potential of Ara-CMCS-EGCG and Cas-CMCS-EGCG solution gradually decreased. The PDI of Ara-CMCS-EGCG and Cas-CMCS-EGCG reached the maximum under condition of 1.8 mg and 3.6 mg EGCG respectively, which indicated that EGCG had strong cross-linking with glycosylated protein.

The embedding efficiency of Ara-CMCS-EGCG increased slowly (Table 1). When the amount of EGCG was 3.6 mg, the embedding efficiency of Ara-CMCS-EGCG reached the maximum. With the amount of EGCG increasing, the embedding efficiency of Cas-CMCS-EGCG decreased rapidly. The embedding rate might be different with different target addition amount (Dridi and Bordenave, 2021). When the EGCG addition amount was 1.0, 1.8, 3.6, 9.0 mg, the EGCG loading amount of Ara-CMCS-EGCG was lower than Cas-CMCS-EGCG. The embedding efficiency of Ara-CMCS-EGCG were higher than that of Cas-CMCS-EGCG. As a whole, Ara-CMCS-EGCG and Cas-CMCS-EGCG had high embedding efficiency. However, when the loading of EGCG was close to saturation, EGCG was not conducive to the stability of whole glycosylated proteins complex solution (Pan et al., 2022).

### 3.3. Fluorescence spectrum characterization of Ara-CMCS-EGCG and Cas-CMCS-EGCG

The fluorescent substance was the premise of the colored substance in the advanced stage of glycosylation. The crosslinking degree and properties of the Ara-CMCS-EGCG and Cas-CMCS-EGCG were analyzed by the changes of the fluorescence intensity. The maximum emission peak wavelengths of Ara-CMCS-EGCG and Cas-CMCS-EGCG were shown in Fig. 3. With the increase of EGCG amount, both Ara-CMCS-EGCG and Cas-CMCS-EGCG showed regular fluorescence quenching phenomenon.

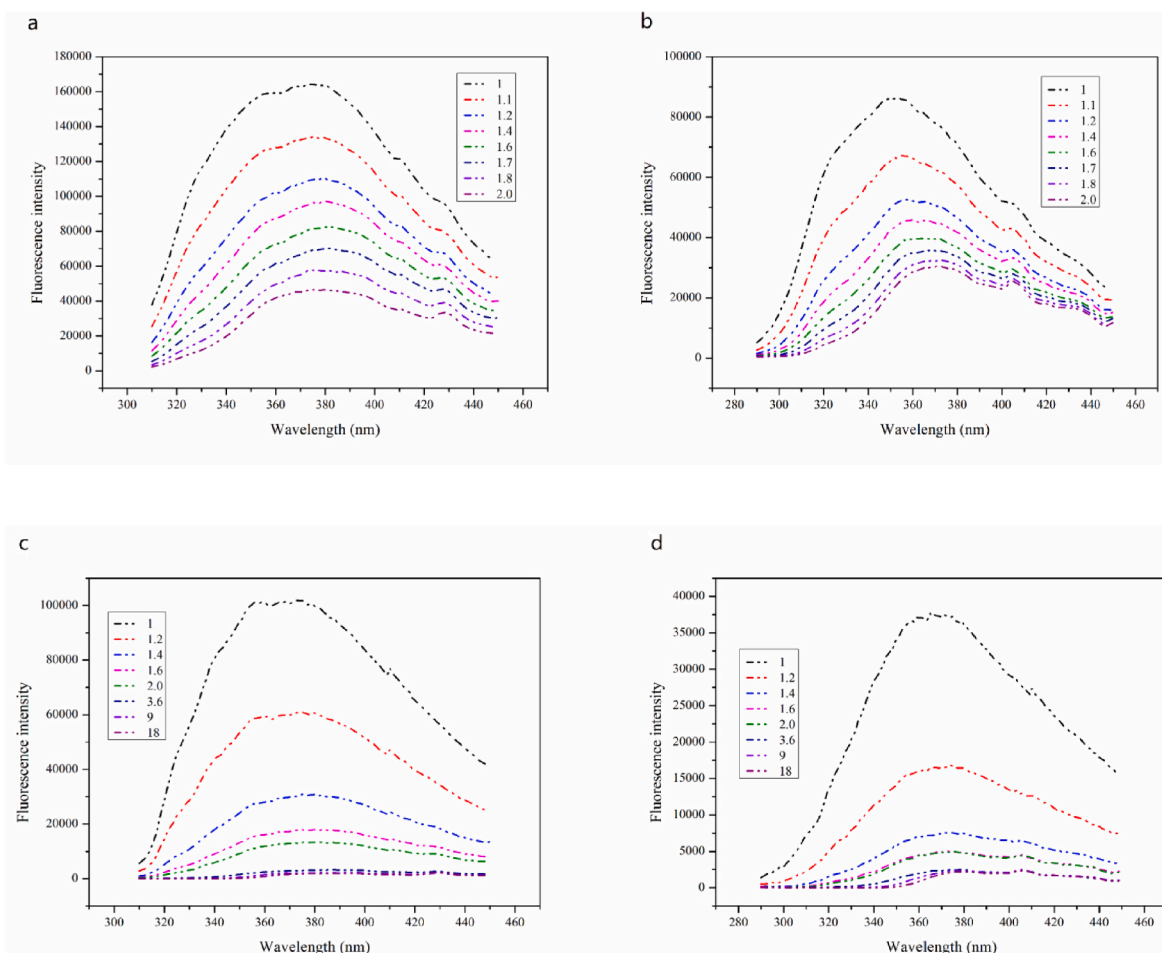


**Fig. 3.** The fluorescence emission spectra of Ara-CMCS-EGCG at 295 nm (a) and 280 nm (b), Cas-CMCS-EGCG at 295 nm (c) and 280 nm (d) with different mass of EGCG addition.

Note: Ara-CMCS-EGCG was EGCG peanut globulin glycosylation copolymer, Cas-CMCS-EGCG was EGCG casein glycosylation copolymer.

It showed that EGCG had mosaic effect on chromogenic amino acid, and the fluorescence of amino acid was weakened. The maximum emission peak of Ara-CMCS-EGCG at 295 nm (Fig. 3. (b)) and Cas-CMCS-EGCG at 280 nm (Fig. 3. (c)) had red shift. The polarity of the surrounding environment of the amino acid residue was exposed to the solution (Huang et al., 2020). The whole fluorescence intensity and quenching effect at 295 nm were higher than those at 280 nm under same EGCG amount, indicating that the tyrosine content of protein complex in solution was higher than that of tryptophan (Mu et al., 2021). The interaction points between EGCG and glycosylated protein were mainly on the tyrosine residue. The above points showed that Ara-CMCS-EGCG and Cas-CMCS-EGCG weakened the fluorescence intensity of amino group on glycosylated protein.

### 3.4. Infrared spectrum characterization of Ara-CMCS-EGCG and Cas-CMCS-EGCG

The chemical structure of the ternary complex of Ara-CMCS-EGCG and Cas-CMCS-EGCG was characterized by FT-IR (Fig. 4.). The results showed that the interaction between EGCG and two glycosylated protein products was mainly hydrogen bond (Yang et al., 2018). The characteristic peak of amide I ( $1600\text{--}1700\text{ cm}^{-1}$ ) was caused by the stretching vibration of C = O compared with the two glycosylated products. The absorption peak of EGCG was significantly weakened near  $1655\text{ cm}^{-1}$ . The peak of Ara-CMCS-EGCG was red shifted. Two characteristic peaks of EGCG at  $1691\text{ cm}^{-1}$  and  $1616\text{ cm}^{-1}$  were disappeared, which might be caused by the interaction between EGCG and C = O = O group of

protein molecular skeleton. In conclusion, there was a hydrogen bond between EGCG and two glycosylated proteins. EGCG could change the structure of glycosylation protein products (Wang et al., 2021).

### 3.5. Fluorescence microstructure characterization of Ara-CMCS-EGCG and Cas-CMCS-EGCG

The composite nanoparticles of Ara-CMCS-EGCG and Cas-CMCS-EGCG were spherical in morphology, uniformed in size and well dispersed under fluorescence microscope (Fig. 5.). At the same magnification, the fluorescence micrograph of Ara-CMCS-EGCG solution was strong, while the fluorescence intensity of Cas-CMCS-EGCG was weak. The fluorescence quenching of casein was stronger than that of peanut globulin. The grafting degree of casein was higher than that of peanut globulin. The surface of Cas-CMCS-EGCG was covered with more carboxymethyl chitosan. The negative charge on the surface of casein complex was less than that of peanut globulin, which tended to be more neutral. The molecular of Cas-CMCS-EGCG mutual repulsion was weak. The Cas-CMCS-EGCG was closely distributed, while the Ara-CMCS-EGCG was relatively sparsely arranged in fluorescence micrograph.

## 4. Conclusion

The encapsulation efficiency and embedding mechanism of EGCG glycosylated peanut globulin nanocomposites (Ara-CMCS-EGCG) and EGCG glycosylated casein nanocomposites (Cas-CMCS-EGCG) were studied. Results revealed that the highest encapsulation efficiency of

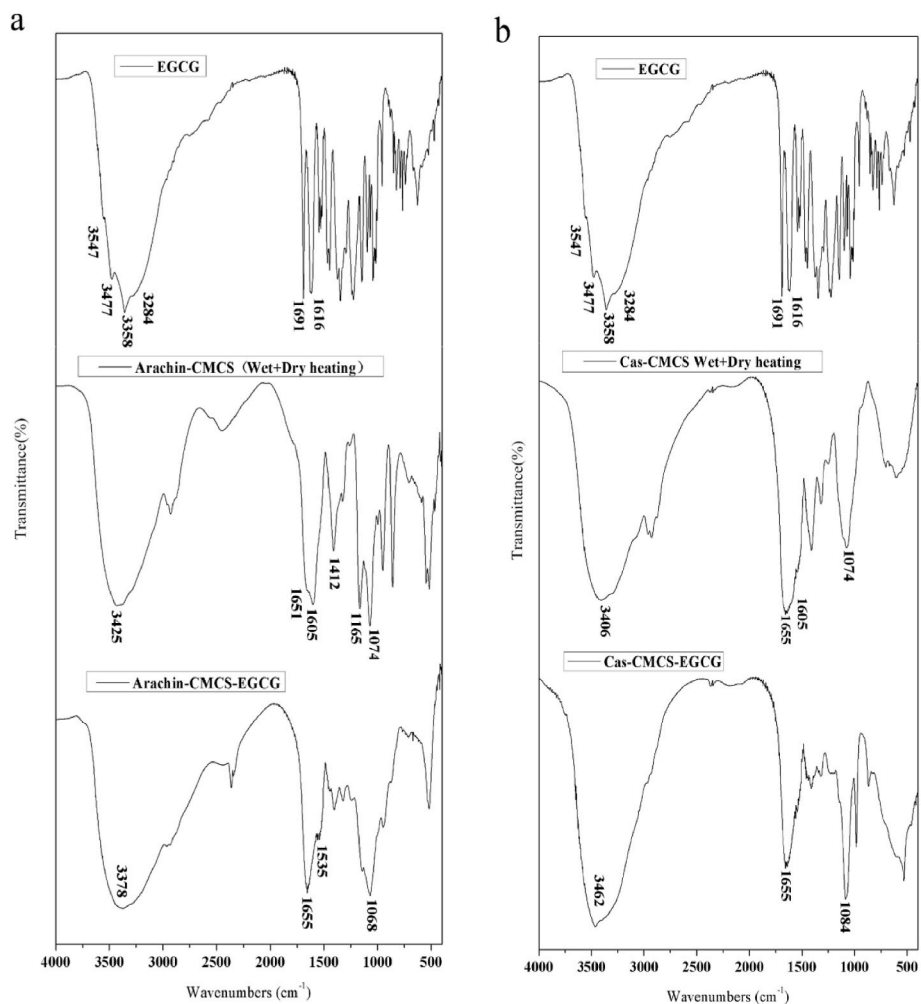


**Fig. 4.** FT-IR spectra of Ara-CMCS-EGCG and Cas-CMCS-EGCG complex.

Note: FT-IR was Fourier transform infrared spectroscopy, Ara-CMCS-EGCG was EGCG peanut globulin glycosylation copolymer, Cas-CMCS-EGCG was EGCG casein glycosylation copolymer.

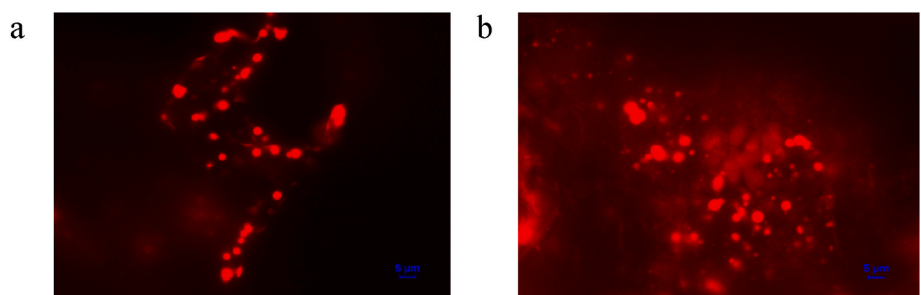


**Fig. 5.** Nanostructures of Ara-CMCS-EGCG (a) and Cas-CMCS-EGCG (b) under the fluorescence microscopy.

Note: Ara-CMCS-EGCG was EGCG peanut globulin glycosylation copolymer, Cas-CMCS-EGCG was EGCG casein glycosylation copolymer.

EGCG could reached to  $93.89 \pm 1.11\%$ . The hydrogen bond between EGCG hydroxyl group and tyrosine and tryptophan of glycosylated protein is mainly non covalent. The fluorescence and dispersion of Ara-CMCS-EGCG are higher than those of Cas-CMCS-EGCG. This study might provide a theoretical basis for EGCG nanocomposites technology and EGCG application in tea beverage and liquid tea food systems.

**CRedit authorship contribution statement**

**Jianyong Zhang:** Investigation, Data curation, Writing – original

draft. **Hongchun Cui:** Investigation, Data curation, Writing – original draft. **Jiahuan Qiu:** Investigation, Data curation, Methodology. **Yixin Zhong:** Investigation, Data curation, Writing – review & editing. **Caiping Yao:** Investigation, review & editing. **Lanying Yao:** Investigation, Data curation, review & editing. **Qunxiong Zheng:** Investigation, review & editing. **Chunhua Xiong:** Conceptualization, Methodology, Supervision.

## Declaration of competing interest

The authors declare the following financial interests/personal relationships which may be considered as potential competing interests: Jianyong Zhang reports financial support was provided by Zhejiang Gongshang University.

## Data availability

Data will be made available on request.

## Acknowledgments

The work is supported by Zhejiang Gongshang University, Tea Research Institute of Chinese Academy of Agricultural Science, and Tea Research Institute of Hangzhou Academy of Agricultural Science; Program of Science and Technology of China Zhejiang Province (No. LGN19B040001), Key Agricultural and Social Development Research Project of China Hangzhou (No. 202203A06).

## References

- Abdelmoneem, M.A., Mahmoud, M., Zaky, A., Helmy, M.W., Sallam, M., Fang, J.Y., Elkhodairy, K.A., et al., 2018. Dual-targeted casein mi-cells as green nanomedicine for synergistic phytotherapy of hepatocellular carcinoma. *J. Contr. Release* 287, 78–93. <https://doi.org/10.1016/j.jconrel.2018.08.026>.
- Chang, C., Nickerson, M.T., 2018. Stability and in vitro release behaviour of encapsulated omega fatty acid-rich oils in lentil protein isolate-based microcapsules. *Int. J. Food Sci. Nutr.* 69 (1), 12–23. <https://doi.org/10.1080/09637486.2017.1336513>.
- Chang, Y., Jiao, Y., Li, D.J., Liu, X.L., Han, H., 2022. Glycosylated zein as a novel nano delivery vehicle for lutein. *Food Chem.* 376, 131927–131935. <https://doi.org/10.1016/j.foodchem.2021.131927>.
- Chen, W.J., Wang, W.J., Ma, X.B., Lv, X.B., Watharkar, R.B., Ding, T., et al., 2019. Effect of pH-shifting treatment on structural and functional properties of whey protein isolate and its interaction with (–)-epigallocatechin-3-gallate. *Food Chem.* 274, 234–241. <https://doi.org/10.1016/j.foodchem.2018.08.106>.
- Dai, W.Z., Ruan, C.C., Zhang, Y.M., Wang, J.J., Han, J., Shao, Z.H., et al., 2020. Bioavailability enhancement of EGCG by structural modification and nanodelivery: a review. *J. Funct. Foods* 65, 103732–103740. <https://doi.org/10.1016/j.jff.2019.103732>.
- Dridi, W., Bordenave, N., 2021. Influence of polysaccharide concentration on polyphenol-polysaccharide interactions. *Carbohydr. Polym.* 274, 118670–118679. <https://doi.org/10.1016/j.carbpol.2021.118670>.
- Du, X.J., Jing, H.J., Wang, L., Huang, X., Mo, L., Bai, X.P., et al., 2022. pH-shifting formation of goat milk casein nanoparticles from insoluble peptide aggregates and encapsulation of curcumin for enhanced dispersibility and bioactivity. *LWT* 154, 112753–112763. <https://doi.org/10.1016/j.lwt.2021.112753>.
- Huang, T.W., Ho, Y.C., Tsai, T.N., Tseng, C.L., Lin, C., Mi, F.L., 2020. Enhancement of the permeability and activities of epigallocatechin gallate by quaternary ammonium chitosan/fucoidan nanoparticles. *Carbohydr. Polym.* 242, 116312–116320. <https://doi.org/10.1016/j.carbpol.2020.116312>.
- Latnikova, A., Jobmann, M.T., 2017. Towards microcapsules with improved barrier properties. *Top. Curr. Chem.* 375, 64–81. <https://doi.org/10.1007/s41061-017-0152-5>.
- Liang, J., Yan, H., Yang, H.J., Kim, H.W., Wan, X.C., Lee, J.H., et al., 2016. Synthesis and controlled-release properties of chitosan/β-Lactoglobulin nanoparticles as carriers for oral administration of epigallocatechin gallate. *Food Sci. Biotechnol.* 25 (6), 1583–1590. <https://doi.org/10.1007/s10068-016-0244-y>.
- Mu, M., Liang, X.Y., Chuan, D., Zhao, S.S., Yu, W., Fan, R.R., et al., 2021. Chitosan coated pH-responsive metal-polyphenol delivery platform for melanoma chemotherapy. *Carbohydr. Polym.* 264, 11800–11810. <https://doi.org/10.1016/j.carbpol.2021.118000>.
- Pan, Y.J., Jin, W.P., Huang, Q.R., 2022. Structure, assembly and application of novel peanut oil body protein extracts nanoparticles. *Food Chem.* 367, 130678–130686. <https://doi.org/10.1016/j.foodchem.2021.130678>.
- Parolia, S., Maley, J., Sarmaynaiken, R., Green, R., Nickerson M., Ghosh, S., 2022. Structure-Functionality of lentil protein-polyphenol conjugates. *Food Chem.* 367, 130603–130612. <https://doi.org/10.1016/j.foodchem.2021.130603>.
- Qiu, J.H., Zheng, Q.X., Fang, L., Wang, Y.B., Min, M., Shen, C., et al., 2018. Preparation and characterization of casein-carrageenan conjugates and self-assembled microcapsules for encapsulation of red pigment from paprika. *Carbohydr. Polym.* 196, 322–331. <https://doi.org/10.1016/j.carbpol.2018.05.054>.
- Shay, R., Keppler, J.K., Schrader, K., Schwarz, K., 2019. Encapsulation of (–)-epigallocatechin-3-gallate (EGCG) in solid lipid nanoparticles for food applications. *J. Food Eng.* 244, 91–100. <https://doi.org/10.1016/j.jfoodeng.2018.09.008>.
- Sieminska-Kuczer, A., Szymanska-Chragot, M., Zdunek, A., 2022. Recent advances in interactions between polyphenols and plant cell wall polysaccharides as studied using an adsorption technique. *Food Chem.* 373, 131487–131497. <https://doi.org/10.1016/j.foodchem.2021.131487>.
- Song, H.D., He, A.J., Guan, X., Chen, Z.Y., Bao, Y.Z., Huang, K., 2022. Fabrication of chitosan-coated epigallocatechin-3-gallate (EGCG)-hordein nanoparticles and their transcellular permeability in Caco-2/HT29 cocultures. *Int. J. Biol. Macromol.* 195, 144–150. <https://doi.org/10.1016/j.jbiomac.2021.12.024>.
- Vesperini, D., Chaput, O., Munier, N., Maire, P., Edwards-Levy, F., Salsac, A.V., et al., 2017. Deformability- and size-based microcapsule sorting. *Med. Eng. Phys.* 48, 68–74. <https://doi.org/10.1016/j.medengphy.2017.06.040>.
- Wang, Q., Cao, J., Yu, H., Zhang, J.H., Yuan, Y.Q., Shen, X.R., et al., 2019. The effects of EGCG on the mechanical, bioactivities, cross-linking and release properties of gelatin film. *Food Chem.* 271, 204–210. <https://doi.org/10.1016/j.foodchem.2018.07.168>.
- Wang, P.Y., Yang, C.T., Chu, L.K., 2021. Differentiating the protein dynamics using fluorescence evolution of tryptophan residue(s): a comparative study of bovine and human serum albumins upon temperature jump. *Chem. Phys. Lett.* 781, 138998–139006. <https://doi.org/10.1016/j.cplett.2021.138998>.
- Wang, Y.P., Ye, A.Q., Hou, Y.Y., Jin, Y.Y., Xu, X.K., Han, J.Z., et al., 2022. Microcapsule delivery systems of functional ingredients in infant formulae: research progress, technology, and feasible application of liposomes. *Trends Food Sci. Technol.* 119, 36–44. <https://doi.org/10.1016/j.tifs.2021.11.016>.
- Yang, J., Mao, L., Yang, W., Sun, C.X., Dai, L., Gao, Y.X., 2018. Evaluation of non-covalent ternary aggregates of lactoferrin, high methylated pectin, EGCG in stabilizing β-carotene emulsions. *Food Chem.* 240, 1063–1071. <https://doi.org/10.1016/j.foodchem.2017.07.127>.
- Zhan, F.C., Youssef, M., Shah, B.R., Li, J., Li, B., 2022. Overview of foam system: natural material-based foam, stabilization, characterization, and applications. *Food Hydrocolloids* 125, 107435–107449. <https://doi.org/10.1016/j.foodhyd.2021.107435>.
- Zhang, E., Xing, R., Liu, S., Qin, Y.K., Li, K.C., Li, P.C., 2019. Advances in chitosan-based nanoparticles for oncotherapy. *Carbohydr. Polym.* 222, 115004–115015. <https://doi.org/10.1016/j.carbpol.2019.115004>.